

Electron-phonon coupling in charge-transfer and crystal-field states of Jahn-Teller CuCl_6^{4-} systems

R. Valiente and F. Rodríguez*

DCITIMAC, Facultad de Ciencias, Universidad de Cantabria, Santander 39005, Spain

(Received 25 March 1999)

In this work we present an octahedral perturbative model to explain the dependence of the crystal-field (CF) and the charge-transfer (CT) energy with respect to structural distortions in Jahn-Teller (JT) CuCl_6^{4-} systems. The method provides a simple way to express the variation of electronic energy to complex distortions of the totally symmetric mode $Q_{a_{1g}}$ and the JT mode Q_θ , as a function of the corresponding electron-vibration coupling constants, $[\partial E/\partial Q_i]_{O_h}$ ($i = Q_{a_{1g}}$ and Q_θ). A value of $9100 \text{ cm}^{-1}/\text{\AA}$ for the linear JT coupling constant A_1 has been obtained for the octahedral ${}^2E_g(x^2-y^2, 3z^2-r^2)$ CF state ($e \otimes E$) from structural correlations along a series of copper compounds. The corresponding JT coupling for the ${}^2T_{1u}(\pi)$ CT state ($e \otimes T$), $A_2 = 3000 \text{ cm}^{-1}/\text{\AA}$, has been derived from hydrostatic pressure measurements performed on the $(\text{C}_3\text{H}_7\text{NH}_3)_2\text{CuCl}_4$ perovskite layer. A noteworthy conclusion of this model is that a redshift of the intense $e_u(\pi) \rightarrow b_{1g}(x^2-y^2)$ CT band is possible in axially elongated CuCl_6^{4-} systems upon anisotropic volume reduction, if the axial distance decreases more rapidly than the equatorial distance by $|\Delta R_{\text{ax}}| > 30|\Delta R_{\text{eq}}|$. These results are discussed in light of recent pressure experiments carried out in wide-gap CT semiconductors of the $A_2\text{CuCl}_4$ family. [S0163-1829(99)02534-5]

I. INTRODUCTION

Linear electron-vibration coupling in O_h transition metal (TM) complexes MX_6 , $X = \text{F}, \text{Cl}, \text{Br}, \text{O}, \text{S}, \text{CN}, \dots$, is a fundamental parameter to understand the optical spectra and the relaxed excited-state equilibrium geometry, as well as to predict structural distortions of the complex induced by uniaxial stress or hydrostatic pressure.¹⁻⁶ In Jahn-Teller (JT) systems such as CuX_6^{4-} , the knowledge of the linear coupling constants $[\partial E/\partial Q_{a_{1g}}]_{O_h}$ and $[\partial E/\partial Q_{\theta,\varepsilon}]_{O_h}$, associated with displacements along the symmetric modes of the O_h complex a_{1g} and the JT active $e_g(Q_\theta, Q_\varepsilon)$, for the crystal-field (CF) and charge transfer (CT) excited states is important. These coupling constants largely determine the ground state and the CT equilibrium geometries. In fact, the first derivative $A_1 = \frac{1}{2} \partial E_{\text{CF}}/\partial Q_{\theta,\varepsilon}$ where E_{CF} is the splitting of the octahedral ${}^2E_g(x^2-y^2, 3z^2-r^2)$ state, plays a crucial role in the $e \otimes E$ JT coupling.⁴⁻⁶ In first-order JT coupling, the CuX_6^{4-} ground-state geometry corresponds to any point of the circumference of radius, $\rho_0 = \sqrt{Q_\theta^2 + Q_\varepsilon^2} = A_1/\mu\omega^2$, in $(Q_\theta, Q_\varepsilon)$ space (Mexican hat potential-energy surface). This means that structures going from the axially elongated octahedron ($Q_\theta = \rho_0, Q_\varepsilon = 0$) to the axially compressed octahedron ($Q_\theta = -\rho_0, Q_\varepsilon = 0$), passing through different tetragonal and rhombic intermediate structures ($Q_\theta \neq 0, Q_\varepsilon \neq 0$), are equally probable. Second-order JT effects of e_g symmetry and anharmonic effects stabilize the axially elongated geometry (D_{4h}) having the tetragonal axis along either z, x , or y with the same probability, i.e., along any minimum of the three potential wells of the warped Mexican hat at $(Q_\theta = \rho_0, Q_\varepsilon = 0)$, $[Q_\theta = -\frac{1}{2}\rho_0, Q_\varepsilon = (\sqrt{3}/2)\rho_0]$ and $[Q_\theta = -\frac{1}{2}\rho_0, Q_\varepsilon = -(\sqrt{3}/2)\rho_0]$, respectively. In that case the JT stabilization energy is $\Delta E = -E_{\text{JT}} \approx -A_1\rho_0/2$. A detailed review of the $e \otimes E$ JT effect in Cu^{2+} complexes can be found elsewhere.⁴⁻⁶

Analogously, the linear coupling constant of the first CT state with respect to octahedral distortions $Q_{a_{1g}}$ and Q_{e_g} are important since they contain valuable information on the variation of the $X^- \rightarrow \text{Cu}^{2+}$ CT energy E_{CT} to JT distortions as well as to isotropic changes of volume. In particular, the knowledge of how E_{CT} depends upon structural distortions is relevant in wide band-gap CT semiconductors like the layered perovskites $A_2\text{CuCl}_4$ ($A = \text{alkylammonium group}$),⁷⁻⁹ as well as many copper oxides,¹⁰⁻¹² given that it is related to the energy gap governing the electrooptical properties of these materials.

The aim of this work is to investigate the electron-vibration coupling associated with the first CF $a_{1g}(3z^2-r^2) \rightarrow b_{1g}(x^2-y^2)$ electronic transition and the first $e_u(\pi) \rightarrow b_{1g}(x^2-y^2)$ CT transition in CuCl_6^{4-} systems. The coupling constants are obtained from structural correlations on the basis of a perturbed octahedral model, and are used to explore how structural changes of the complex affect the CT and CF states in JT Cu^{2+} systems. The results of this work are applied to predict energy shifts as a function of the complex distortion. Recent pressure experiments on $A_2\text{CuCl}_4$ will also be discussed within this model.^{7,13}

$A_2\text{CuCl}_4$ layer compounds show a large variety of interesting physical phenomena associated with the antiferrodistortive structure displayed by the JT axially elongated CuCl_6^{4-} complexes (Fig. 1). They are two-dimensional ferromagnets with $T_C = 10 \text{ K}$ (Refs. 14 and 15) and have attracted interest as material related to high- T_C superconductors and as organic-inorganic hybrid layered systems. The color of these crystals, which is determined by the optical window formed by the first $e_u(\pi) \rightarrow b_{1g}(x^2-y^2)$ CT band placed at 26000 cm^{-1} , and the CF band of highest energy around $12000\text{--}17000 \text{ cm}^{-1}$, strongly depends on the CuCl_6^{4-} coordination geometry.¹⁶⁻²⁰ Therefore structural changes of the complex geometry induced either by tempera-

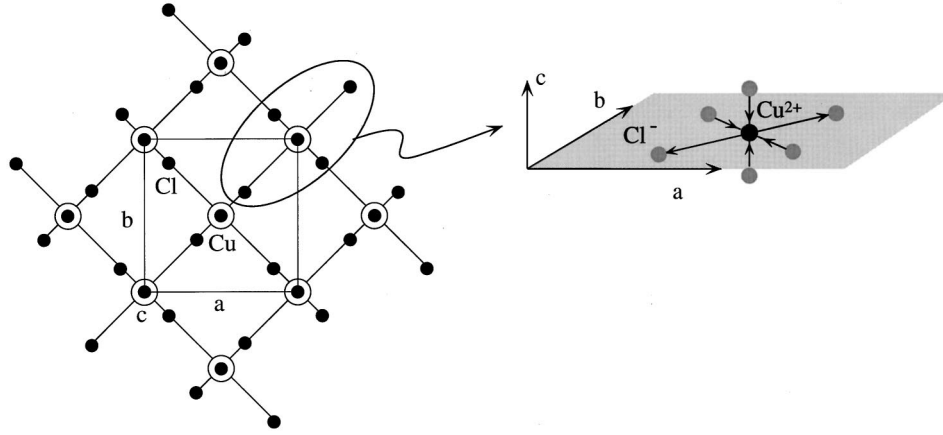


FIG. 1. Schematic view of the A_2CuCl_4 perovskite layer. The alternating $CuCl_4^{2-}$ units form an antiferrodistortive structure associated with the orthogonal orientation of the in-plane Cu-Cl bonds of neighboring Cu. This structure yields a real $CuCl_6^{4-}$ coordination geometry of nearly D_{4h} symmetry, where the in-plane equatorial Cl ligand of one Cu acts as axial ligand of the nearest Cu. The two equatorial Cl along c are terminal ligands. The orthorhombic a , b , and c cell vectors are indicated.

ture or pressure may lead to interesting thermochromic or piezochromic effects. The thermochromism exhibited by the $[(C_2H_5)_2NH_2]_2CuCl_4$ crystal is an example of this behavior.²¹ In this work we investigate the influence of structural changes of $CuCl_6^{4-}$ on the optical properties in both CT and CF domains. This knowledge is of value in establishing guidelines to be followed for the synthesis of Cu^{2+} -based optical materials.

II. EXPERIMENT

Single crystals of $(C_2H_7NH_3)_2CuCl_4$ examined in pressure experiments, were grown from aqueous solution as described elsewhere.²⁰ The hydrostatic pressure experiments were done in a diamond-anvil cell (High Pressure Diamond Optics, Inc.), using paraffin oil as the pressure transmitter to prevent crystal hydration. The absorption spectra have been obtained with an implemented single beam spectrometer^{13,22} able to measure optical densities in the 0–5 range. Microsamples of $80 \times 80 \times 2 \mu m^3$ were necessary for obtaining suitable CT spectra of the layered perovskites (absorption coefficient, $k \approx 5 \times 10^4 cm^{-1}$). The pressure was measured through the R -line shift of ruby chips introduced in the hydrostatic cavity. The ruby luminescence was excited with the 568-nm line of a Coherent I-302 Krypton Laser.

III. RESULTS AND DISCUSSION

A. Perturbed octahedral model for $CuCl_6^{4-}$

The perturbative model developed here deals with the dependence of the CF and CT transitions as a function of the $CuCl_6^{4-}$ distortion. The model consists of expanding the octahedral $CuCl_6^{4-}$ Hamiltonian in terms of the normal coordinates Q_i ($i = a_{1g}, e_g, e_g$), rather than in terms of bond distances R_i ($i = ax, eq, eq_2$). This procedure is advantageous since it expresses separately CF and CT contributions and most parameters involved in the model can be obtained experimentally through structural correlations. In addition, it provides information concerning the electron-vibration cou-

pling associated, not only with the electronic ground state, but also the first $Cl^- \rightarrow Cu^{2+}$ CT state both from variations of volume, $[\partial E_{CT}/\partial Q_{a_{1g}}]_{Q_\theta}$, and from tetragonal distortions at constant volume, $[\partial E_{CT}/\partial Q_\theta]_{Q_{a_{1g}}}$. A conclusion derived from this model is that a redshift of the first CT energy in $CuCl_6^{4-}$ is possible upon anisotropic reduction of the complex volume. Moreover, it predicts a CT redshift even for complex distortions involving a reduction of all Cu-Cl distances. In particular, these estimates foresee a pressure-induced redshift for the first CT band in A_2CuCl_4 in the event of an axial distance decrease while the equatorial Cu-Cl distance is unmodified: $\Delta R_{ax} < 0$, $\Delta R_{eq} = 0$. This structural variation upon pressure was in fact proposed by Moritomo and Tokura in $(C_2H_5NH_3)_2CuCl_4$ from Raman measurements,⁷ and thus is in agreement with the CT redshift observed in this crystal and in other A_2CuCl_4 systems.¹³

The proposed perturbative model is similar to Kaplyanskii's method for describing piezospectroscopic shifts in optical centers.²³ In general, the variation of the $CuCl_6^{4-}$ complex Hamiltonian with respect to distortions of the octahedral symmetry can be expanded as a function of the octahedral normal coordinates Q_i as

$$H = H_0 + \Delta H = H_0 + \sum_i \left[\frac{\partial H}{\partial Q_i} \right]_{Q_j=0} Q_i, \quad (1)$$

where H_0 is the octahedral Hamiltonian and $[\partial H/\partial Q_i]_{O_h}$ is the Hamiltonian derivative with respect to a complex distortion described by the normal coordinate Q_i (i denotes the corresponding O_h irreducible representation). Although this expansion could also be done as a function of the six bond distances R_i the use of normal coordinates is advantageous for analyzing the relevant energy derivatives of the perturbed Hamiltonian ΔH . In fact, the corresponding Hamiltonian representation matrices $\langle \Delta H \rangle$ are traceless for all modes except for the totally symmetric a_{1g} , if the electronic states involved in the transition are like in the present case (2E_g and ${}^2T_{1u}$), orbital doublets or triplets (Fig. 2):

TABLE I. Relevant structural and spectroscopic parameters for several Cu^{2+} chlorides. R_{eq} and R_{ax} are the equatorial and axial Cu-Cl distances of the CuCl_6^{4-} complexes. The first three compounds correspond to square-planar CuCl_4^{2-} complexes. ΔR_{eq} denotes the orthorhombic degree of the nearly tetragonal complex. $R_{\text{eq}} = (R_1 + R_2)/2$ and $\Delta R_{\text{eq}} = (R_1 - R_2)/2$ where R_1 and R_2 are the short Cu-Cl distances defining the equatorial plane of the complex. The tetragonal and rhombic normal coordinates Q_θ and Q_ε are related to these distances as $Q_\theta = (2/\sqrt{3})(R_{\text{ax}} - R_{\text{eq}})$ and $Q_\varepsilon = 2\Delta R_{\text{eq}}$; $R_0 = \frac{1}{3}(R_1 + R_2 + R_3) = \frac{1}{3}(2R_{\text{eq}} + R_{\text{ax}})$ is the average Cu-Cl distance. The three (ε_1 , ε_2 , and ε_3) parameters are the crystal-field energies associated with transitions $a_{1g}(3z^2 - r^2) \rightarrow b_{1g}(x^2 - y^2)$, $b_{2g}(xy) \rightarrow b_{1g}(x^2 - y^2)$, and $e_g(xz, yz) \rightarrow b_{1g}(x^2 - y^2)$, respectively, obtained from the electronic spectra. $\varepsilon_1 = \Delta_e$ represents the splitting of the parent octahedral $e_g(x^2 - y^2, 3z^2 - r^2)$ levels. The experimental data were taken from references given in the last row. Compounds are written with the commonly used names.

Compound	R_{eq} (Å)	R_{ax} (Å)	ΔR_{eq} (Å)	$\varepsilon_1 = \Delta_e$ (cm $^{-1}$)	$\varepsilon_2 = 10Dq$ (cm $^{-1}$)	ε_3 (cm $^{-1}$)	Q_θ (Å)	Q_ε (Å)	ρ (Å)	Ref.
$\text{C}_{42}\text{H}_{56}\text{N}_2\text{O}_2\text{CuCl}_4$	2.26			16 600	12 200	14 000				28,29,30
(creatinium) $_2\text{CuCl}_4$	2.25			16 500	12 300	14 000				34,30
(<i>nmp</i> H $_2$) CuCl_4	2.27			16 900	12 500	14 500				31,32,33
[Pt(NH $_3$) $_4$] CuCl_4	2.287	3.257	0.016	14 300	10 900	13 100	1.120	0.032	1.120	41,42
(<i>cyclam</i> H $_4$) CuCl_6	2.296	3.175	0.005	13 400	11 100	12 400	1.015	0.010	1.015	18
(<i>n</i> -PrNH $_3$) $_2\text{CuCl}_4$	2.29	3.04	0	11 300	12 300	13 500	0.87	0	0.87	27,38
(<i>Et</i> NH $_3$) $_2\text{CuCl}_4$	2.281	2.975	0.004	11 130	12 390	13 290	0.801	0.008	0.801	37,38
(<i>Met</i> NH $_3$) $_2\text{CuCl}_4$	2.290	2.907	0.007	11 090	12 110	13 210	0.712	0.014	0.712	39,40
(3-Cl- <i>an</i>) $_8(\text{CuCl}_6)\text{Cl}_3$	2.327	2.827	0.051	9000	10 400	12 100	0.577	0.101	0.586	43,44,25
CsCuCl_3	2.318	2.776	0.037	8300	10 000	12 930	0.529	0.074	0.534	35,36

$$\begin{aligned} \Delta E_{\text{CF}}(a_{1g} \rightarrow b_{1g}) &= \left[\frac{\partial E(a_{1g} - b_{1g})}{\partial Q_\theta} \right]_{Q_{a_{1g}}=0} Q_\theta \\ &= 4 \left[\frac{\partial E_{\text{JT}}}{\partial Q_\theta} \right]_{Q_{a_{1g}}=0} Q_\theta, \\ \Delta E_{\text{CT}}(e_u \rightarrow b_{1g}) &= \left\{ 2 \left[\frac{\partial E_{\text{JT}}}{\partial Q_\theta} \right] \pm \frac{1}{3} \left[\frac{\partial E_L}{\partial Q_\theta} \right] \right\}_{Q_{a_{1g}}=0} Q_\theta \\ &+ \left[\frac{\partial E_{\text{CT}}(t_{1u} - e_g)}{\partial Q_{a_{1g}}} \right]_{Q_\theta=0} Q_{a_{1g}}. \quad (4) \end{aligned}$$

The \pm sign corresponds to the elongated (+) and compressed (−) situations. Note that the splitting of the parent octahedral $e_g(x^2 - y^2, 3z^2 - r^2)$ MO's does not depend on $Q_{a_{1g}}$ but it does depend on Q_θ (and Q_ε). A similar situation occurs for the mainly ligand t_{1u} MO's. Therefore the present equations for the energy shift of the first CT and CF transitions are expressed as a function of three parameters, two of which can be experimentally obtained from structural correlations.^{13,20} These parameters represent the splitting derivative of the t_{1u} ligand orbitals (E_L) and the e_g metal orbitals ($4E_{\text{JT}}$) with respect to the tetragonal coordinate, $Q_\theta = (2/\sqrt{3})(R_{\text{ax}} - R_{\text{eq}})$, and can be derived from spectroscopic data of a copper compound series, where the local structure around Cu^{2+} is known from x-ray diffraction (Table I and Fig. 3), and the pressure results shown in Fig. 4. The third parameter $[\partial E_{\text{CT}}/\partial Q_{a_{1g}}]_{Q_\theta=0}$ represents the variation of the first CT energy, $E_{\text{CT}} = E(t_{1u}) - E(e_g)$, of the octahedral complex with respect to $Q_{a_{1g}} = \sqrt{6}\{[(R_{\text{ax}} + 2R_{\text{eq}})/3] - R_0\}$, where $R_0 = 2.53$ Å is the average Cu-Cl distance. The lack of correlations between the CT spectra and the metal-ligand distances in O_h TM complexes precludes any effort to derive the $[\partial E_{\text{CT}}/\partial Q_{a_{1g}}]_{Q_\theta=0}$ parameter from experimental data.

However, it can be estimated from MS- $X\alpha$ calculations performed on CuCl_6^{4-} of D_{4h} symmetry for different values of R_{ax} and R_{eq} .²⁴ It is worth noting here that although calculations provide suitable values of the electronic structure of the complex, they underestimate the variation of the JT energy with respect to the tetragonal distortion in comparison to the results shown in Fig. 3.²⁵ The value $[\partial E_{\text{CT}}/\partial Q_{a_{1g}}]_{Q_\theta=0} = -13\,500 \text{ cm}^{-1}/\text{Å}$, employed in this work has been obtained from calculations performed on CuCl_6^{4-} for two different geometries ($Q_\theta > 0$ and $Q_\theta < 0$) (Ref. 24) by extracting the tetragonal contribution to the total CT energy. This value is similar to estimates based on the variation of electrostatic potential created by the complex at the ligand and metal sites. That variation is known to be mainly responsible for the CT shifts induced by variations of R in O_h complexes.¹⁹ Therefore the R -dependence of the CT energy obtained on the basis of this assumption is

$$\begin{aligned} \frac{\partial E_{\text{CT}}}{\partial Q_{a_{1g}}} &\approx \frac{+e}{\sqrt{6}} \frac{\partial V_{L-M}}{\partial R} = + \frac{1}{6} \frac{e^2}{R^2} (-2.67q_M + q_L) \\ &= -14\,000 \text{ cm}^{-1}/\text{Å} \end{aligned}$$

for an average Cu-Cl distance $R_0 = 2.53$ Å, and ionic charges $q_L = -1$ for the ligand and $q_M = 2$ for the metal, respectively. V_{L-M} is the electrostatic potential difference at the ligand and metal sites. The similarity between this and the MS- $X\alpha$ value makes it a proper estimate of this unknown parameter.

As previously mentioned, the remaining two parameters of Eq. (3) can be derived from the experimental data shown in Figs. 3 and 4. The variation of the first CF band in CuCl_6^{4-} as a function of $\rho = \sqrt{Q_\theta^2 + Q_\varepsilon^2}$ is shown in Fig. 3. The corresponding spectroscopic and structural data are collected in Table I. The wide structural range covered by the compound series allows us to estimate the JT energy derivative with respect to the Q_θ coordinate $\partial E_{\text{JT}}/\partial Q_\theta$ which rep-

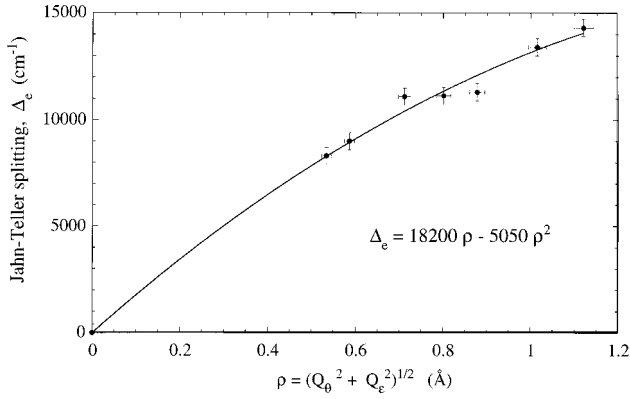


FIG. 3. Spectroscopic and structural correlations in CuCl_6^{4-} complexes. The plot shows the variation of the tetragonal splitting, $\Delta_e = 4E_{\text{JT}} = E[b_{1g}(x^2 - y^2)] - E[a_{1g}(3z^2 - r^2)]$, with the structural distortion coordinate, $\rho = [Q_\theta^2 + Q_\epsilon^2]^{1/2}$, measured along the series of copper compounds given in Table I. The full line is the least-square fitting to a quadratic function. The linear electron-vibration Jahn-Teller coupling derived from this curve is $A_1 = 9100 \text{ cm}^{-1}$.

resents half the electron-vibration coupling constant $-A_1/2$. The extrapolated derivative obtained from Fig. 3 is

$$\begin{aligned} \left[\frac{\partial E_{\text{CF}}}{\partial \rho} \right]_{\rho=0} &= \left[\frac{\partial E_{\text{CF}}}{\partial Q_\theta} \right]_{Q_\epsilon=Q_\theta=0} \\ &= 4 \left[\frac{\partial E_{\text{JT}}}{\partial Q_\theta} \right]_{Q_\epsilon=Q_\theta=0} = 18200 \text{ cm}^{-1}/\text{\AA}. \end{aligned}$$

Note that this value is higher than the CT isotropic contribution $[\partial E_{\text{CT}}/\partial Q_{a_{1g}}]_{Q_\theta=0} = -13500 \text{ cm}^{-1}/\text{\AA}$, thus stressing the relevance of the JT contribution to the CT shifts. The linear electron-vibration coupling constant between the octahedral degenerate 2E_g ground state and the vibrational $e_g(Q_\theta, Q_\epsilon)$ mode $E \otimes e$ is then $A_1 = -[\partial E({}^2B_{1g})]/\partial Q_\theta = \frac{1}{2} \partial E_{\text{CF}}/\partial Q_\theta = 9100 \text{ cm}^{-1}/\text{\AA}$. The JT coupling constant obtained through this method is similar to $A_1 = 7000 \text{ cm}^{-1}/\text{\AA}$ found by Reinen and Hitchman in CuCl_6^{4-} formed in the triclinic compound $(3\text{-Cl-an})_8[\text{CuCl}_6]\text{Cl}_4$.²⁵ The discrepancy is due to the procedure employed by the authors for estimating A_1 as twice the ratio of the JT energy derived from the electronic spectra to the CuCl_6^{4-} distortion in such a crystal. As indicated in Fig. 3, that method provides A_1 values lower than the present one derived as $A_1 = [\frac{1}{2} \partial \Delta_e(\rho)/\partial \rho]_{\rho=0}$.

It must be observed that the JT distortion $\rho_0 = A_1/\mu\omega^2$,^{4,5} deduced for an isolated CuCl_6^{4-} complex taking $\mu_{\text{Cl}} = 5.9 \times 10^{-23} \text{ g}$ and $\omega = 4.2 \times 10^{13} \text{ s}^{-1}$,^{18,20} is $\rho_0 = 0.18 \text{ \AA}$. Note that this value is significantly shorter than the experimental JT distortion found for CuCl_6^{4-} along the series shown in Table I stressing the influence of the crystal anisotropy in the JT equilibrium geometry. Therefore the present estimates suggest that a reduction of the JT distortion induced by pressure from the zero pressure values $\rho_0 = 1.0\text{--}0.6 \text{ \AA}$ to $\rho_0 = 0.1\text{--}0.3 \text{ \AA}$ at high pressure is likely.

B. Charge-transfer band assignment

The JT contribution to the CT energy coming from the ligand t_{1u} MO cannot be obtained from structural correla-

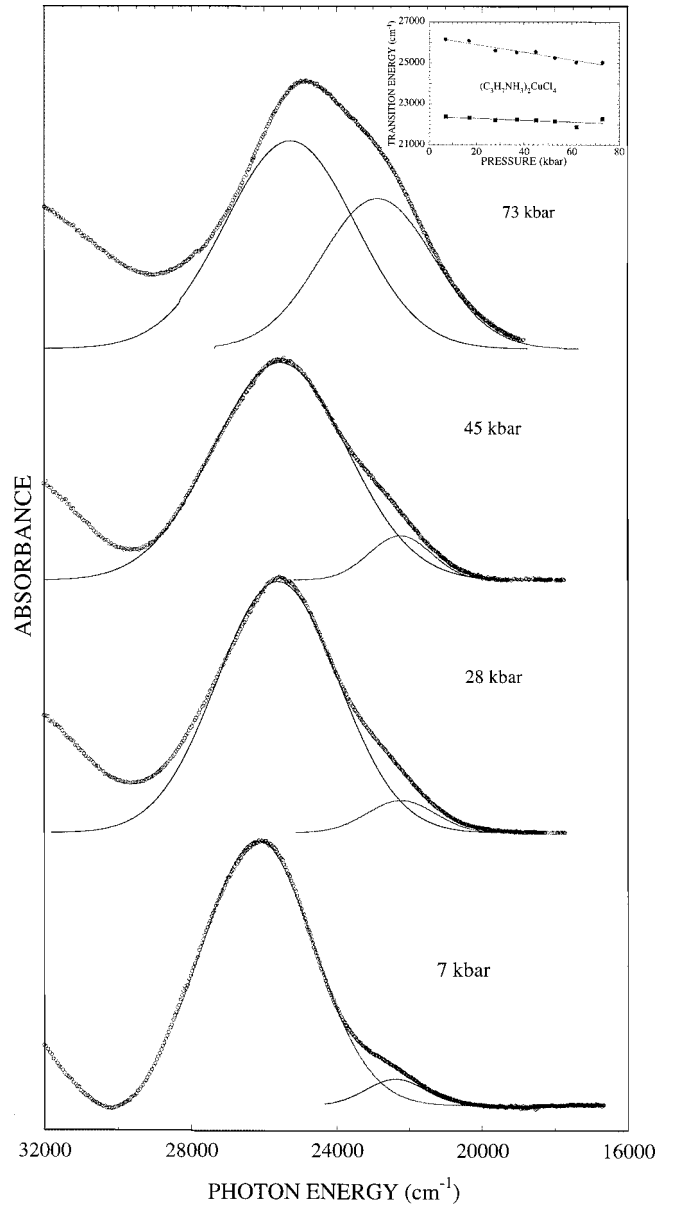


FIG. 4. Variation of the absorption band associated with the first $\text{Cl}^- \rightarrow \text{Cu}^{2+}$ CT transition $e_u(\pi) \rightarrow b_{1g}(x^2 - y^2)$ with hydrostatic pressure in the $(\text{C}_3\text{H}_7\text{NH}_3)_2\text{CuCl}_4$ perovskite layer. Note the presence of a small shoulder at low energies (see text for assignment). The spectra have been fitted to the sum of two Gaussians which are shown (full lines) together with the absorption data (points). The inset shows the variation of the peak energy of the two Gaussians with pressure. The straight lines correspond to least-square linear fitting of the data: $E_{\text{CT1}} = 26300 - 18.5P$ and $E_{\text{CT2}} = 22400 - 4.2P$. Units in cm^{-1} (E) and Kbars (P). Crystal size: $80 \times 80 \times 2 \mu\text{m}^3$.

tions due to the lack of CT spectra in pure compounds. However hydrostatic pressure experiments performed on $(\text{C}_3\text{H}_7\text{NH}_3)_2\text{CuCl}_4$ and shown in Fig. 4, allows us (i) to clarify the origin of the two components observed in the first CT band, and (ii) to estimate the parameter $[\partial E_L/\partial Q_\theta]$. In fact, the intense component at 26000 cm^{-1} corresponds to the D_{4h} -allowed $e_u \rightarrow b_{1g}$ CT transition of the axially elongated CuCl_6^{4-} complex,^{16,20,26} while we assign the weak shoulder to the $a_{2u} \rightarrow b_{1g}$ CT transition. Although this latter transition is forbidden in D_{4h} , small deviations of the complex symmetry toward D_{2h} makes it partially allowed. The

presence of the weak component at 22400 cm^{-1} is likely to reflect the actual D_{2h} symmetry (nearly D_{4h}) of the CuCl_6^{4-} complex in $(\text{C}_3\text{H}_7\text{NH}_3)_2\text{CuCl}_4$.²⁷ This interpretation is strongly supported by the pressure behavior of the two components. First, the weak $a_{2u} \rightarrow b_{1g}$ component ($a_{2u} \rightarrow a_{1g}$ in D_{2h}) of the CT band increases with pressure. Second, both components shift to lower energies and their splitting continuously reduces with pressure. Both features agree with the structural model proposed by Moritomo and Tokura,⁷ for explaining the pressure-induced disappearance of the antiferrodistortive structure in $(\text{C}_2\text{H}_5\text{NH}_3)_2\text{CuCl}_4$. The authors suggest an evolution of the complex structure from an elongated octahedron to an octahedron or a nearly octahedral geometry. This structural transformation must bring the two $e_u \rightarrow b_{1g}$ and $a_{2u} \rightarrow b_{1g}$ CT components into $t_{1u} \rightarrow e_g$ in the hypothetical octahedral limit, where both components should have the same energy and intensity. Nevertheless, an evolution of CuCl_6^{4-} to an octahedron is not possible due to the JT effect.⁴⁻⁶ The present results can be concealed with the disappearance of the antiferrodistortive structure if we assume that the main effect of pressure on the local structure of CuCl_6^{4-} is to reduce the axial distance and the out-of-layer equatorial Cu-Cl distance, leading to an orthorhombic complex with a radius $\rho_0 \approx 0.18\text{ \AA}$, close to the octahedron $\rho_0 = 0$.

Therefore the results of Fig. 4 support the structural evolution foreseen from Raman measurements,⁷ and also confirm the CT assignment for this low energy shoulder proposed elsewhere.²⁶

C. Energy shift analysis

According to the CT band assignment, we can now make a rough estimate of the electron-vibration coupling constant, $A_2 = \frac{2}{3} [\partial E_L / \partial Q_\theta]_{Q_{a_{1g}}} = 3000\text{ cm}^{-1}/\text{\AA}$, from the CT band splitting observed at atmospheric pressure, $\Delta E(e_u - a_{2u}) = E_L = 3900\text{ cm}^{-1}$ in $(\text{C}_3\text{H}_7\text{NH}_3)_2\text{CuCl}_4$ and the corresponding tetragonal distortion, $Q_\theta = 0.87\text{ \AA}$. Although this procedure underestimates the actual derivative at $Q_\theta = 0$, it does not affect the conclusions derived throughout the present analysis. Replacing these values in Eq. (4) we obtain

$$\begin{aligned} \Delta E_{\text{CT}} &= \left\{ 2 \frac{\partial E_{\text{JT}}}{\partial Q_\theta} \pm \frac{1}{3} \frac{\partial E_L}{\partial Q_\theta} \right\}_{Q_{a_{1g}}} Q_\theta + \left[\frac{\partial E_{\text{CT}}}{\partial Q_{a_{1g}}} \right]_{Q_\theta=0} Q_{a_{1g}} \\ &= (9100 \pm 1500) Q_\theta - 13\,500 Q_{a_{1g}}. \end{aligned} \quad (5)$$

Before analyzing the CT shift for different distortions of the CuCl_6^{4-} octahedron on the basis of Eq. (5), it is worthwhile to underline that the JT contribution to the first CT energy $E_{\text{CT}} = 26\,000\text{ cm}^{-1}$ in $(\text{C}_3\text{H}_7\text{NH}_3)_2\text{CuCl}_4$ is approximately $\Delta_{\text{JT}} = 2E_{\text{JT}} + \frac{1}{3}E_L = 5650 + 1300 = +6950\text{ cm}^{-1}$ (Table I and Fig. 4). This value represents 27% of the total energy, thus confirming the importance of JT effect to the CT energy in CuCl_6^{4-} . Given that this term is directly related to structural deviations from the octahedral symmetry, distortions of the $A_2\text{CuCl}_4$ layer crystals yielding a decrease of the initial tetragonal symmetry of CuCl_6^{4-} must affect significantly both the first CT and CF energies.

From Eq. (5), we conclude that the CT shift is different for elongated and compressed D_{4h} complexes. In the former case, $\Delta E_{\text{CT}} = 10\,600 Q_\theta - 13\,500 Q_{a_{1g}}$ while it is $7600 Q_\theta - 13\,500 Q_{a_{1g}}$ in the latter case. However, a similar contribution to the CT shift is found for a tetragonal and an isotropic distortion described in terms of normal coordinates in both situations. As is well known, Eq. (5) also predicts a CT blueshift upon an isotropic compression of CuCl_6^{4-} : $Q_{a_{1g}} < 0$ and $Q_\theta = 0$. Nevertheless, either a blueshift or a redshift is possible whenever an elongated ($Q_\theta > 0$) or a compressed ($Q_\theta < 0$) tetragonal distortion at constant volume takes place. This result agrees with findings on CuCl_6^{4-} for these two geometries through MS- $X\alpha$ calculations.²⁴

Interestingly, the structural distortion attained in pressure experiments performed on $A_2\text{CuCl}_4$ is worthwhile. The pressure-induced axially compression of CuCl_6^{4-} is also accompanied by a reduction of the complex volume: $Q_\theta < 0$ and $Q_{a_{1g}} < 0$. This means that $\Delta E_{\text{CT}} = -10\,600 |Q_\theta| + 13\,500 |Q_{a_{1g}}|$, and therefore there is a competition between both isotropic and tetragonal distortions tending to shift the CT band to higher and lower energies, respectively. There will be either a redshift or a blueshift depending on whether $|Q_\theta|$ is greater or smaller than $1.27 |Q_{a_{1g}}|$, respectively. In terms of Cu-Cl distances, the CT shift can be written as $\Delta E_{\text{CT}} = +1200 \Delta R_{\text{ax}} - 34\,300 \Delta R_{\text{eq}}$, for elongations while $\Delta E_{\text{CT}} = -2250 \Delta R_{\text{ax}} - 30\,800 \Delta R_{\text{eq}}$ for compressions. A salient conclusion of this analysis is that a CT redshift associated with the reduction of all Cu-Cl distances is possible in elongated CuCl_6^{4-} . Such a redshift, however, is not possible in an axially compressed complex since the two coefficients are negative, i.e., the JT contribution to the CT shift coming from the metal and ligand orbitals have opposite signs (Fig. 2). The positive value of $[\partial E_{\text{CT}} / \partial R_{\text{ax}}]_{R_{\text{eq}}}$ indicates that the JT contribution to the CT band shift associated with the shortening of the axially elongated Cu-Cl bond is more important than the blueshift contribution due to volume reduction. This result is noteworthy since it predicts a CT redshift upon $\Delta R_{\text{ax}} < 0$ and $\Delta R_{\text{eq}} < 0$ if the variation of the equatorial distance is shorter than 3.5% the axial distance variation ($|\Delta R_{\text{eq}}| < 0.035 |\Delta R_{\text{ax}}|$). Therefore JT distortions play a crucial role in the CT energy shift.

According to the proposed structural evolution for CuCl_6^{4-} upon pressure, the redshift of about 1000 cm^{-1} observed along the $A_2\text{CuCl}_4$ series can be accounted for within this model if the main effect of pressure is to reduce the Cu-Cu distance within the crystal layer (i.e., the orthorhombic a and b lattice parameters) but keeping the four short equatorial Cu-Cl bonds at $R_{\text{eq}} = 2.29\text{ \AA}$. With regard to the local structure of Cu^{2+} , this evolution leads to a reduction of R_{ax} , and therefore to a CT redshift according to the previous analysis. Given that a variation of about $\Delta R_{\text{ax}} \sim 0.7\text{ \AA}$ is expected in the explored pressure range, the CT shift would be similar to the measured one according to Eq. (5). It must be emphasized, however, that although the present analysis provides suitable values of the CT shift rate in distorted CuCl_6^{4-} complexes, quantitative estimates from this perturbative model must be taken with caution for distortions $Q_\theta > 0.5\text{ \AA}$ (Fig. 3). Precise quantitative estimates for highly distorted complex like most of the known Cu^{2+} complexes

deserve electronic structure calculations as a function of R_{ax} and R_{eq} around the tetragonal equilibrium geometry of CuCl_6^{4-} . Work along this line is currently in progress.

IV. CONCLUSIONS

In this work we have developed a perturbative octahedral-complex model to predict energy shift of the CT and CF bands in JT CuCl_6^{4-} systems induced by isotropic and tetragonal structural distortions. This model is advantageous since the shift rates can be described in terms of linear electron-vibration coupling parameters whose values can be obtained from structural correlations. In addition, second-order effects like configuration interaction between different octahedral states, are negligible within this model. The shift rate estimates and the electron-vibration coupling constants

associated with the JT effect for the ground state A_1 ($e \otimes E$) and the CT state A_2 ($e \otimes T$) provide a simple way of explaining the pressure-induced CT redshift as well as the structural variation of the Cu^{2+} environment related to the progressive disappearance of the antiferrodistortive structure observed along the $(\text{C}_n\text{H}_{2n+1}\text{NH}_3)_2\text{CuCl}_4$ ($n = 1-3$) series in hydrostatic pressure experiments.

ACKNOWLEDGMENTS

Fruitful discussions with Professor M. Moreno, Professor J. A. Aramburu, and Professor M. T. Barriuso (University of Cantabria), and Professor M. Hitchman (University of Tasmania) are acknowledged. This work was supported by Caja Cantabria, the Vicerrectorado de Investigación de la Universidad de Cantabria and the CICYT (Project No. PB95-0581).

*Author to whom correspondence should be addressed. Electronic address: rodriguf@ccaix3.unican.es

¹M. D. Sturge, *Solid State Phys.* **20**, 91 (1967).

²W. B. Fowler, *Physics of Color Centers* (Academic, New York, 1968).

³A. B. P. Lever, *Inorganic Electronic Spectroscopy* (Elsevier, New York, 1984).

⁴D. Reinen and M. Atanasov, *Magn. Reson. Rev.* **15**, 167 (1991).

⁵M. A. Hitchman, *Comments Inorg. Chem.* **15**, 197 (1994).

⁶J. S. Griffith, *The Theory of Transition-Metal Ions* (Cambridge University Press, Cambridge, England, 1980).

⁷Y. Moritomo and Y. Tokura, *J. Chem. Phys.* **101**, 1763 (1994).

⁸G. C. Papavassiliou, *Prog. Solid State Chem.* **25**, 125 (1997).

⁹T. Yoshinari, T. Nanba, S. Shimanuki, M. Fujisawa, T. Matsuyama, M. Ikezawa, and K. Aoyagi, *J. Phys. Soc. Jpn.* **61**, 2224 (1992).

¹⁰M. K. Kelly, P. Barboux, J. M. Tarascon, D. E. Aspnes, W. A. Bonner, and P. A. Morris, *Phys. Rev. B* **38**, 870 (1988).

¹¹P. Adler and A. Simon, *Z. Phys. B* **85**, 197 (1991).

¹²J. M. Leng, J. M. Ginder, W. E. Farneth, S. I. Shah, and A. J. Epstein, *Phys. Rev. B* **43**, 10 582 (1991).

¹³R. Valiente, Ph.D. thesis, University of Cantabria, 1998.

¹⁴L. J. De Jongh and A. R. Miedema, *Adv. Phys.* **23**, 1 (1974).

¹⁵T. Sekine, T. Okuno, and K. Awaga, *Chem. Phys. Lett.* **249**, 201 (1996).

¹⁶S. R. Desjardins, D. E. Wilcox, R. L. Musselman, and E. I. Solomon, *Inorg. Chem.* **26**, 288 (1987).

¹⁷R. D. Willett, F. H. Jardine, I. Rouse, R. J. Wong, C. P. Landee, and M. Numata, *Phys. Rev. B* **24**, 5372 (1981).

¹⁸R. G. McDonald and M. A. Hitchman, *Inorg. Chem.* **28**, 3996 (1989).

¹⁹M. Moreno, M. T. Barriuso, and J. A. Aramburu, *Appl. Magn. Reson.* **3**, 283 (1992).

²⁰R. Valiente and F. Rodríguez, *J. Phys. Chem. Solids* **57**, 571 (1996).

²¹D. R. Bloomquist, M. R. Pressprich, and R. D. Willett, *J. Am. Chem. Soc.* **110**, 7391 (1988).

²²B. A. Moral and F. Rodríguez, *Rev. Sci. Instrum.* **66**, 5178 (1995).

²³A. A. Kaplyanskii, *Opt. Spectrosc.* **16**, 329 (1964).

²⁴J. A. Aramburu and M. Moreno, *J. Chim. Phys.* **86**, 871 (1989).

²⁵D. Reinen and M. A. Hitchman, *Z. Phys. Chem. (Munich)* **200**, 11 (1997).

²⁶B. Baticle, F. Rodríguez, and R. Valiente, *Radiat. Eff. Defects Solids* **135**, 89 (1995).

²⁷F. Barendregt and H. Schenk, *Physica (Amsterdam)* **49**, 465 (1970).

²⁸H. C. Nelson, S. H. Simonsen, and G. W. Watt, *J. Chem. Soc. Chem. Commun.* **1979**, 632.

²⁹M. J. Riley and M. A. Hitchman, *Inorg. Chem.* **28**, 3926 (1989).

³⁰R. G. McDonald and M. A. Hitchman, *Inorg. Chem.* **25**, 3273 (1986).

³¹R. L. Harlow, W. J. Wells, G. W. Watt, and S. H. Simonsen, *Inorg. Chem.* **13**, 2106 (1974).

³²M. A. Hitchman and P. Cassidy, *Inorg. Chem.* **18**, 1745 (1979).

³³P. Cassidy and M. A. Hitchman, *J. Chem. Soc. Chem. Commun.* **1975**, 837.

³⁴M. R. Udupa and B. Krebs, *Inorg. Chim. Acta* **33**, 241 (1979).

³⁵A. W. Suetler, R. A. Jacobseon, and R. E. Rundle, *Inorg. Chem.* **28**, 3996 (1966).

³⁶R. Laiho, M. Natarajan, and M. Kaira, *Phys. Status Solidi A* **15**, 311 (1973).

³⁷J. P. Steadman and R. D. Willett, *Inorg. Chim. Acta* **4**, 367 (1970).

³⁸M. A. Hitchman and P. Cassidy, *Inorg. Chem.* **17**, 1682 (1978).

³⁹I. Pabst, H. Fuess, and W. Bats, *Acta Crystallogr., Sect. C: Cryst. Struct. Commun.* **43**, 413 (1987).

⁴⁰S. R. Desjardins, K. W. Penfield, S. L. Cohen, R. L. Musselman, and E. I. Solomon, *J. Am. Chem. Soc.* **105**, 4590 (1983).

⁴¹B. Morosin, P. Fallon, and J. S. Valentine, *Acta Crystallogr., Sect. B: Struct. Crystallogr. Cryst. Chem.* **31**, 2220 (1975).

⁴²W. E. Hatfield and T. S. Piper, *Inorg. Chem.* **3**, 841 (1964).

⁴³P. J. Ellis, H. C. Freeman, M. A. Hitchman, D. Reinen, and B. Wagner, *Inorg. Chem.* **33**, 1249 (1994).

⁴⁴H. Stratemeir, B. Wagner, E. R. Krausz, R. Linder, H. H. Schmidtke, J. Pebler, W. E. Hatfield, L. Haar, D. Reinen, and M. A. Hitchman, *Inorg. Chem.* **33**, 2320 (1994).